

1
2
3
4
5
6
7
8
9
10
11
12
13
14
15
16
17
18
19
20
21

**An octopamine-specific GRAB sensor reveals a monoamine relay
circuitry that boosts aversive learning**

Mingyue Lv^{1,2,3}, Ruyi Cai^{1,3}, Renzimo Zhang^{1,3,4,5}, Xiju Xia^{1,3,6}, Xuelin Li^{1,3}, Yipan Wang^{1,3}, Huan
Wang^{1,3}, Jianzhi Zeng^{1,3,7}, Yifei Xue⁸, Lanqun Mao⁸, Yulong Li^{1,3,4,5,6,7,9*}

¹State Key Laboratory of Membrane Biology, School of Life Sciences, Peking University,
Beijing 100871, China

²State Key Laboratory of Brain and Cognitive Science, Institute of Biophysics, Chinese
Academy of Sciences, Beijing 100101, China.

³PKU-IDG/McGovern Institute for Brain Research, Beijing 100871, China

⁴Yuanpei College, Peking University, Beijing 100871, China

⁵Peking-Tsinghua Center for Life Sciences, Academy for Advanced Interdisciplinary
Studies, Peking University, Beijing 100871, China

⁶Peking University–Tsinghua University–National Institute of Biological Sciences Joint
Graduate Program, Academy for Advanced Interdisciplinary Studies, Peking University,
Beijing 100871, China

⁷Institute of Molecular Physiology, Shenzhen Bay Laboratory, Shenzhen 518107, China

⁸College of Chemistry, Beijing Normal University, Beijing 100875, China

⁹Chinese Institute for Brain Research, Beijing 102206, China.

*Manuscript correspondence: Yulong Li (yulongli@pku.edu.cn)

ORIGINAL UNEDITED MANUSCRIPT

22 ABSTRACT

23 Octopamine (OA), analogous to norepinephrine in vertebrates, is an essential
24 monoamine neurotransmitter in invertebrates that plays a significant role in various
25 biological functions, including olfactory associative learning. However, the spatial and
26 temporal dynamics of OA *in vivo* remain poorly understood due to limitations
27 associated with the currently available methods used to detect it. To overcome these
28 limitations, we developed a genetically encoded GPCR activation-based (GRAB) OA
29 sensor called GRAB_{OA1.0}. This sensor is highly selective for OA and exhibits a robust
30 and rapid increase in fluorescence in response to extracellular OA. Using GRAB_{OA1.0},
31 we monitored OA release in the *Drosophila* mushroom body (MB), the fly's learning
32 center, and found that OA is released in response to both odor and shock stimuli in an
33 aversive learning model. This OA release requires acetylcholine (ACh) released from
34 Kenyon cells, signaling via nicotinic ACh receptors. Finally, we discovered that OA
35 amplifies aversive learning behavior by augmenting dopamine-mediated punishment
36 signals via Oct β 1R in dopaminergic neurons, leading to alterations in synaptic
37 plasticity within the MB. Thus, our new GRAB_{OA1.0} sensor can be used to monitor OA
38 release in real-time under physiological conditions, providing valuable insights into the
39 cellular and circuit mechanisms that underlie OA signaling.

40
41 **Key words:** octopamine, dopamine, GRAB sensor, learning and memory

42 43 INTRODUCTION

44 Octopamine (OA) is an essential monoamine neurotransmitter in invertebrates,
45 analogous to norepinephrine (NE) in vertebrates[1, 2]. In vertebrates, OA is classified
46 as a trace amine and is thought to be associated with emotional responses[3-5]. In
47 invertebrates, OA plays a role in various physiological processes, including the
48 sleep-wake cycle, flight, ovulation, aggression, and associative learning[6-27].

49 In *Drosophila melanogaster*, OA has been implicated in regulating both learning and
50 memory, particularly in the formation of short-term associative memories of an
51 odor-conditioned stimulus (CS) paired with either an appetitive sugar reward or an
52 aversive electrical body shock as the unconditioned stimulus (US). Moreover, studies
53 have shown that mutants lacking tyramine β hydroxylase (T β H), the rate-limiting
54 enzyme for OA biosynthesis, have an impaired ability to acquire appetitive
55 memory[19]. Furthermore, stimulation of octopaminergic neurons (OANs) can replace

56 sugar presentation during conditioning and lead to the formation of short-term
57 appetitive memory[20, 21]. However, studies regarding aversive conditioning have
58 yielded conflicting results. For example, some studies found normal performance in
59 T β H mutants[19, 28], while other studies found impaired performance when
60 compared to wild-type (WT) flies[29].

61 In the *Drosophila* brain, the mushroom body (MB) is the main center for olfactory
62 learning[30-33] and consists primarily of Kenyon cells (KCs), with their dendrites
63 residing in the calyx and their axon bundles projecting through the peduncle to form
64 the α/β lobe, α'/β' lobe and γ lobe[34-36]. Studies have shown that OA signaling via
65 the β -adrenergic-like OA receptor Oct β 1R is required for aversive memory formation
66 in the MB[25]. In addition to its role in short-term memory, OA released from the
67 anterior paired lateral (APL) neurons has been shown to modulate intermediate-term
68 aversive memory by acting on KCs via Oct β 2R[23]. Together, these findings suggest
69 that OA indeed plays a key role in aversive learning and memory in *Drosophila*.
70 However, there are still many unresolved issues regarding the spatiotemporal
71 dynamics of OA release and the specific role OA plays in aversive learning that
72 warrant further investigations.

73 Our relatively limited understanding of how OA functions spatially and temporally
74 during learning is primarily due to limitations in current detection methods. Traditional
75 methods, such as microdialysis-coupled biochemical analysis[37-39], offer high
76 specificity but low temporal resolution and complex sampling procedures, especially
77 in invertebrates. On the other hand, electrochemical techniques like fast-scan cyclic
78 voltammetry (FSCV) enable rapid monitoring of endogenous OA release[40, 41], but
79 they cannot distinguish between OA and other structurally similar neurotransmitters,
80 particularly its biological precursor tyramine (TA), which differs from OA by only one
81 hydroxyl group and also serves as an important monoamine in invertebrates[2].

82 To overcome these limitations, we developed a novel G protein-coupled receptor
83 (GPCR) activation-based (GRAB) OA sensor, utilizing the *Drosophila* Oct β 2R as the
84 sensing module and circularly-permuted enhanced green fluorescent protein
85 (cpEGFP) as the reporter; we call this sensor GRAB_{OA1.0} (hereafter referred to as
86 OA1.0). We found that this sensor is highly specific to OA, has sub-second kinetics,
87 and exhibits a peak increase in fluorescence of approximately 660% in response to
88 OA. Using OA1.0, we then measured spatiotemporal changes of OA in the *Drosophila*
89 MB in response to odor and shock stimuli. Our findings reveal that the release of OA
90 in the MB promotes the release of dopamine (DA), which increases the fly's
91 perception of the US, thereby facilitating aversive learning.

92

93 RESULTS

94 Development and characterization of GRAB_{OA1.0}

95 To monitor octopamine (OA) release *in vivo* with high specificity, sensitivity and
96 spatiotemporal resolution, we employed a well-established strategy[42-53] to develop
97 a genetically encoded GPCR activation-based (GRAB) sensor for OA using EGFP to
98 report an increase in extracellular OA through an increase in fluorescence intensity.
99 First, we inserted the conformationally sensitive cpEGFP into the third intracellular
100 loop (ICL3) of the β -adrenergic-like OA receptor Oct β 2R. Next, we systematically
101 screened the position of the cpEGFP and optimized the linker residues between the
102 GPCR and cpEGFP using site-directed mutagenesis. We then mutated the residues
103 near the ligand binding pocket of Oct β 2R to further optimize the performance of the
104 OA sensor. Specifically, we found that introducing at the L7.38V and I7.41M
105 substitutions produced an increasing response to OA, and we named the GRAB_{OA1.0}
106 (OA1.0) sensor (Fig. 1A, B and Fig. S1).

107 When expressed in HEK293T cells, OA1.0 trafficked to the plasma membrane and
108 produced a peak change in fluorescence ($\Delta F/F_0$) of ~660% in response to 100 μ M OA
109 (Fig. 1C). To measure the sensor's kinetics, we used a rapid perfusion system to
110 locally apply OA followed by the OA receptor antagonist epinastine (Ep), and we
111 measured the change in fluorescence using high-speed line scanning. The data were
112 then fitted to obtain an on-rate (τ_{on}) and off-rate (τ_{off}) of approximately 0.02 s and
113 1.40 s, respectively (Fig. 1D). We also measured the spectral properties of OA1.0
114 using both one-photon (1P) and two-photon (2P) excitation, which revealed excitation
115 peaks at ~500 nm and ~920 nm, respectively, and an emission peak at ~520 nm (Fig.
116 1E), similar to those of other commonly used green fluorescent probes. To confirm
117 that OA1.0 does not activate signaling pathways downstream of Oct β 2R (thus not
118 affecting cellular physiology), we measured β -arrestin and Gs pathway activation
119 using the Tango assay[54], a cell-based method that quantifies GPCR activation
120 through β -arrestin recruitment, and the red cAMP sensor RFlamp, respectively. Cells
121 expressing OA1.0 exhibited negligible β -arrestin-dependent signaling compared to
122 cells expressing WT Oct β 2R, even at high concentrations of OA (Fig. 1F, left).
123 Moreover, cells expressing OA1.0 had significantly lower downstream Gs coupling
124 compared to cells expressing WT Oct β 2R (Fig. 1F, right).

125 With respect to its specificity, we found that the OA1.0 signal induced by OA was
126 abolished by Ep, and the application of several other neurotransmitters did not

127 produce a detectable change in fluorescence (Fig. 1G, left). Next, we measured the
128 response of OA1.0 to various concentrations of OA, as well as the structurally similar
129 transmitters tyramine (TA), dopamine (DA) and norepinephrine (NE). We found that
130 OA1.0 has an ~40-fold higher affinity for OA ($EC_{50} = \sim 200$ nM) compared to TA (EC_{50}
131 $= \sim 8000$ nM), and showed a negligible response to DA and NE at all tested
132 concentrations (Fig. 1G, right). However, the utilization of the FSCV method for OA
133 detection does not offer such robust specificity, as we observed significant
134 interference from DA and NE in OA detection despite the relatively minor disruption
135 from TA (Fig. 1H).

136 To evaluate the specificity of OA1.0 *in vivo*, we generated transgenic flies expressing
137 OA1.0 in the MB (30y-GAL4-driven) and then sequentially applied DA, TA, OA and Ep
138 to the fly brain while performing 2P imaging. We found that neither DA nor TA induced
139 an obvious response, while OA elicited a robust response in OA1.0 fluorescence (with
140 a peak $\Delta F/F_0$ of ~100%) that was blocked by Ep (Fig. 1I and J). Together, these data
141 demonstrate that OA1.0 can reliably measure the dynamics of OA release with high
142 specificity for OA.

143 **OA1.0 can report endogenous OA release signals *in vivo***

144 To further characterize the release of endogenous OA *in vivo*, we used *Drosophila*
145 expressing OA1.0 in the MB (MB247-LexA-driven), which receives projections from
146 several pairs of OANs, including ventral unpaired median a2 (VUMa2) neurons,
147 ventral paired median 3 (VPM3) neurons, VPM4 neurons, VPM5 neurons, and APL
148 neurons[23, 55]. To induce the release of endogenous OA in the MB, we applied local
149 electrical stimuli at 30 Hz and observed an incremental increase in fluorescence with
150 an increasing number of stimuli, and this response was eliminated by Ep (Fig. 2A-2D).
151 Moreover, the response was specific to OA, as no detectable response to electrical
152 stimuli was measured in flies lacking T β H in the OANs (Tdc2-GAL4-driven) (Fig. 2C
153 and D). When we applied 50 electrical stimuli at a frequency of 100 Hz, we measured
154 τ_{on} and τ_{off} rates of ~0.6 s and ~9.4 s, respectively (Fig. 2E).

155 To monitor the release of OA in response to the direct activation of OANs *in vivo*, we
156 optogenetically activated OANs (Tdc2-GAL4-driven) in flies expressing
157 CsChrimson-mCherry while simultaneously imaging OA1.0 expressed in the MB
158 (MB247-LexA-driven) (Fig. 2F, 2G). We found that activating OANs induced a
159 transient increase in OA1.0 fluorescence in the $\gamma 1$ - $\gamma 5$ compartments of the MB, with
160 the magnitude of the OA1.0 response dependent on the number of light pulses
161 applied; moreover, the peak responses were similar among all five γ compartments

162 (Fig. 2H and I). Importantly, the response for 100 pulses stimulation was blocked in all
163 five compartments by Ep, confirming the sensor's specificity (Fig. 2H and I). We then
164 measured the kinetics of the response using the γ 3 compartment as an example and
165 found that a single pulse of 635-nm laser evoked a measurable increase in OA1.0
166 fluorescence, with τ_{on} and τ_{off} values of \sim 0.34 s and \sim 5.90 s, respectively (Fig. 2J).
167 Taken together, these results show that OA1.0 can be used *in vivo* to monitor
168 endogenous OA release with high spatiotemporal resolution, high specificity, and high
169 sensitivity.

170 **OA1.0 can detect physiologically evoked OA release in the MB of living flies**

171 The conflicting findings regarding the role of OA in aversive olfactory learning[19, 28,
172 29] highlight the need to better understand whether OA release can be activated by
173 odor and/or an aversive stimulus such as electric body shock, which can represent
174 either the CS or the US in this type of learning. To address this question, we
175 expressed OA1.0 in the *Drosophila* MB (MB247-LexA-driven) and found that both
176 odorant application and electric body shock induced a time-locked increase in OA1.0
177 fluorescence in all five γ compartments, with no difference observed among the
178 various compartments (Fig. 3A-C). In contrast, we found no detectable response to
179 either odorant application or electrical shock in flies in which we knocked down T β H
180 expression in OANs or in flies which OAN activity was suppressed by expressing the
181 inward rectifying potassium channel Kir2.1. As an internal control, direct application of
182 OA still elicited a robust OA1.0 response in both models (Fig. S2).

183 **OA1.0 reveals that KC activity is both necessary and sufficient for OA release in** 184 **the *Drosophila* MB**

185 Next, to examine the mechanism underlying OA release in the MB, we attempted to
186 identify the neurons and pathways that regulate OAN activity. Although previous
187 connectomic analyses showed that KCs, the principal neurons in the MB, are the
188 primary cells upstream of OANs (Fig. S3)[56, 57], the functional inputs that drive OA
189 release are currently unknown. Given that KCs release the excitatory neurotransmitter
190 acetylcholine (ACh)[58], we perfused ACh onto the γ lobe of the MB and observed an
191 increase in OA1.0 fluorescence that was prevented by the nicotinic ACh receptor
192 (nAChR) antagonist mecamylamine (Meca). Moreover, we found no increase in
193 OA1.0 fluorescence when other neurotransmitters such as 5-hydroxytryptamine
194 (5-HT), glutamate (Glu), DA and γ -aminobutyric acid (GABA) were applied in the
195 presence of Meca (Fig. 3D).

196 Because perfusion of exogenous ACh lacks cell-type specificity, we used

197 optogenetics to determine whether selectively activating KCs (R13F02-GAL4-driven)
198 is sufficient to induce OA release in the MB. Consistent with our perfusion
199 experiments, we found that optogenetically activating KCs caused an increase in
200 OA1.0 fluorescence that was blocked by Meca but not the muscarinic ACh receptor
201 antagonist tiotropium (Fig. 3E). Moreover, there is no obvious light-induced OA
202 release in transgenic flies with UAS-CsChrimson but without KC-GAL4
203 (R13F02-GAL4) (Fig. S4A), ruling out the unspecific effect due to the leaky
204 expression of channelrhodopsin[59]. Together, these results suggest that ACh release
205 from KCs serves as the excitatory signal that drives OA release via nAChRs in the γ
206 lobe of the MB.

207 To determine whether KCs are required for activating OANs in the MB, we generated
208 transgenic flies expressing both OA1.0 and the inhibitory DREADD (designer
209 receptors exclusively activated by designer drugs) hm4Di[60-62], and found that both
210 odor- and shock-induced OA1.0 signals were abolished when KCs activity was
211 suppressed by the hm4Di agonist deschloroclozapine (DCZ)[63] (Fig. 3F). Meanwhile,
212 the DCZ application showed no significant effect on stimuli-induced OA signals in flies
213 without hm4Di (Fig. S4B). Thus, KC activity is both necessary and sufficient for OA
214 release from OANs in the MB.

215 **OA regulates aversive learning behavior and related synaptic plasticity**

216 To examine the biological significance of OA release triggered by odorant application
217 and body shock, we measured aversive learning and the coincident time window in
218 flies lacking either OA synthesis or OAN activity. Previous research has demonstrated
219 that the coincidence between the CS and the US is essential for effectively forming
220 associations in aversive learning; furthermore, it has been reported that 5-HT
221 bi-directionally regulates the coincidence time window[64]. We found that both T β H
222 mutant flies and OAN-silenced flies expressing Kir2.1 had significantly reduced
223 learning performance compared to WT flies (Fig. 4A and B). Moreover, unlike flies
224 lacking neuronal tryptophan hydroxylase (Trhn), the rate-limiting enzyme in 5-HT
225 biosynthesis, which have a significantly shortened coincident time window compared
226 to control flies, the coincident time window was unchanged in T β H mutants (Fig. S5).
227 These results suggest that OA plays a key and specific role in aversive learning ability
228 in *Drosophila*.

229 Given that synaptic plasticity is fundamental to the neuronal basis of learning, the
230 regulation of synaptic plasticity by OAN activity after odor-shock pairing is a potential
231 mechanism underlying the observed aversive learning results. Previous

232 electrophysiological recordings or Ca^{2+} imaging studies in the mushroom body output
233 neuron (MBON) innervating the $\gamma 1$ compartment (MBON- $\gamma 1pedc$) suggested that
234 pairing an odorant with dopaminergic reinforcement induces synaptic depression
235 between KCs and the MBON[65-67]. This synaptic depression is correlated with
236 decrease ACh release from KCs[64, 68]. Thus, we used the GRAB_{ACh3.0} sensor
237 (ACh3.0)[45] to monitor the ACh release in the γ lobe of the MB (MB247-LexA-driven)
238 (Fig. 4C-4E). By comparing the odor-evoked ACh release measured before and after
239 odor-shock pairing in control flies, we observed significant synaptic depression in the
240 $\gamma 1$, $\gamma 2$ and $\gamma 3$ compartments (Fig. S6), the three compartments known to transmit
241 information to MBONs associated with approach behavior[69]. We then examined the
242 extent of ACh release depression following odor-shock pairing in flies expressing
243 Kir2.1 in the OANs. Our results revealed significant reductions in ACh release
244 depression (i.e., less synaptic depression) in the CS+ response, specifically in the $\gamma 1$
245 and $\gamma 2$ compartments compared to control flies (Fig. 4F), indicating impaired synaptic
246 plasticity during learning in OAN-silenced flies. In contrast, OAN-silenced flies and
247 control flies showed similar ACh release patterns in response to CS- in all of the γ
248 compartments, indicating that OA is specifically required for learning (Fig. 4G). Taken
249 together, these results suggest that OA plays an essential role in modulating the
250 change in synaptic plasticity induced by odor-shock pairing, thereby amplifying the
251 aversive learning behavior.

252 **OA regulates aversive learning by modulating US processing via Oct β 1R** 253 **expressed on dopaminergic neurons**

254 Synchronization between the CS and the US is required for aversive learning;
255 specifically, information regarding the CS is conveyed by projection neurons to the
256 calyx of the MB for processing by KCs, while information regarding the US is
257 conveyed by dopaminergic neurons (DANs) to the MB lobes for subsequent
258 processing[70]. Consequently, we investigated the specific role of OA in aversive
259 learning. We expressed the calcium sensor GCaMP6s in KCs (MB247-LexA-driven)
260 to measure calcium signals in the calyx, providing information regarding the dynamics
261 of CS processing (Fig. 5A1). The results indicated that OAN-silenced flies exhibited
262 similar KC calcium signals in response to odorant application compared to the control
263 flies (Fig. 5A2 and A4). As anticipated, shock stimuli induced small calcium signals in
264 the KCs of the calyx, and no significant differences were observed between
265 OAN-silenced flies and the corresponding control flies (Fig. 5A3 and A4). Additionally,
266 we expressed the GRAB_{DA2m} (DA2m) sensor [47] in the MB (R13F02-LexA-driven) to
267 measure DA release in the γ lobe, thus capturing the dynamics of US processing (Fig.

268 5B1). We found that shock-induced DA release in the γ lobe was significantly reduced
269 in OAN-silenced flies (Fig. 5B3 and B4). Moreover, odor stimuli induced small DA
270 transients in the γ lobe, and no significant differences were observed between
271 OAN-silenced flies and the corresponding control flies (Fig. 5B2 and B4). Together,
272 these findings suggest that OAN activity modulates US processing, but not CS
273 processing, during aversive learning.

274 To eliminate potential developmental influences on our observations regarding the
275 effect of OA on DA release in response to the US, we applied the OA receptor
276 antagonist Ep to the fly's brain and found that the same individual fly exhibited a
277 significant reduction in shock-induced DA release along the γ lobe compared before
278 and after the Ep treatment (Fig. 5C, left and middle). Previous studies showed that
279 short-term aversive memory formation requires OA signaling via Oct β 1R[25]; we
280 therefore specifically knocked down Oct β 1R expression in DANs (TH-GAL4-driven)
281 using RNAi (Fig. 5C, right) to examine whether OA directly affects DA release and
282 found a significant decrease in DA release compared to controls (Fig. 5C, left and
283 right). Based on these results, we then examined whether knocking down Oct β 1R
284 expression in DANs affects synaptic plasticity and/or learning. Similar to our results
285 obtained with OAN-silenced flies (see Fig. 4), we found significant differences in the
286 degree of KC synaptic depression in response to CS+ in both the γ 1 and γ 2
287 compartments of Oct β 1R-knockdown flies compared to control flies. In contrast, we
288 found no significant differences in the γ 3, γ 4, or γ 5 compartments in response to CS+,
289 or in any γ compartment in response to CS- (Fig. 6A-6E). To further test the role of
290 Oct β 1R expressed in DANs in learning behaviors, we assessed the learning ability of
291 Oct β 1R-knockout flies and Oct β 1R-knockdown flies at the behavioral level. Our
292 results show that, similar to synaptic plasticity, both genotypes of flies displayed
293 significantly impaired learning compared to control flies (Fig. 6F). Taken together,
294 these results support a model in which OA boosts aversive learning via Oct β 1R in
295 DANs, which enhances the punitive US signals to modulate synaptic plasticity in KCs
296 (Fig. 6G).

297 DISCUSSION

298 Here, we developed a new genetically encoded fluorescent sensor called GRAB_{OA1.0}
299 to detect OA release with high selectivity, sensitivity, and spatiotemporal resolution
300 both *in vitro* and *in vivo*. We then used this tool to perform the first detailed study of
301 the spatial and temporal dynamics of OA during aversive learning in *Drosophila*. We
302 found that ACh released from KCs activates OANs, triggering OA release via nAChRs.

303 Notably, we also observed that ACh released from KCs is required for OA release in
304 response to both the CS and the US during aversive learning. Furthermore, by
305 integrating other genetically encoded fluorescent sensors (namely, GRAB_{DA2m} and
306 GRAB_{ACh3.0} to monitor DA and ACh, respectively), we discovered that OA increases
307 shock-induced DA release via Oct β 1R, which in turn regulates the corresponding
308 changes in synaptic plasticity in the MB, ultimately facilitating aversive learning.

309 **Advantages of OA1.0 over other methods for measuring OA**

310 Compared to other methods used to measure OA, OA1.0 offers several advantages.
311 First, OA1.0 exhibits high specificity for OA over most neurotransmitters such as TA,
312 DA and NE. This is particularly important for detecting OA in the presence of other
313 structurally similar molecules, as electrochemical tools like FSCV cannot distinguish
314 between OA and other chemicals, as shown here (Fig. 1H) and in previous
315 studies[39-41]. Second, OA1.0 offers sub-second kinetics and is genetically encoded,
316 allowing for the non-invasive monitoring of octopaminergic activity *in vivo* with a high
317 recording rate. In contrast, microdialysis has relatively low temporal resolution and
318 requires the placement of a relatively large probe, making it unsuitable for use in small
319 model organisms such as *Drosophila*. Capitalizing on these advantages, we used
320 OA1.0 to monitor OA release *in vivo* in response to a variety of stimuli, gaining new
321 insights into the functional role of OA.

322 Importantly, OA1.0 can also be expressed in other animal models, including mammals,
323 opening up new opportunities to monitor OA dynamics in a wide range of species. In
324 mammals, OA is classified as a trace amine and exerts its activity through trace
325 amine-associated receptors (TAARs). TAAR1, in particular, has been implicated as a
326 key regulator of monoaminergic and glutamatergic signaling in brain regions relevant
327 to schizophrenia, as demonstrated in knockout and overexpression models in
328 rodents[71, 72]. However, studying TAAR1 is challenging due to the presence of
329 various endogenous ligands, including the trace amines β -phenylethylamine (PEA),
330 TA, and OA, as well as the monoamine neurotransmitters DA, 5-HT, and NE[73]. Thus,
331 the development of robust tools like OA1.0 that selectively monitor a given trace
332 amine will advance our understanding of specific TAAR-mediated biological effects.
333 Additionally, this strategy can be employed to develop sensors for detecting other key
334 trace amines, providing valuable information regarding these chemicals' dynamics
335 under both physiological and pathological conditions.

336 **OA plays a key role in associative learning**

337 OA was initially believed to play a role only in appetitive learning, but not in aversive

338 learning, in invertebrates such as *Drosophila*, honeybees, and crickets[19, 28, 74, 75].
339 However, several studies suggest that OA may indeed be involved in aversive
340 learning, albeit without completely understanding the underlying mechanisms and
341 spatiotemporal dynamics[23, 25, 29]. Schwaerzel et al. first showed that OA has the
342 selective role in *Drosophila*, reporting that T β H mutants had impaired appetitive
343 learning but normal aversive learning[19]. However, it is important to note that the
344 T β H mutants used by Schwaerzel et al. were a mixture of homozygous and
345 hemizygous T β H^{M18} flies regardless of sex, as the localization of T β H was to the X
346 chromosome and the homozygous T β H^{M18} females were sterile. Subsequently, Iliadi
347 et al. found that both homozygous T β H^{M18} males and females performed impaired
348 aversive conditioning compared to WT flies and heterozygous T β H^{M18} females[29].
349 Drawing on these previous reports, we used homozygous T β H^{M18} males and females
350 and obtained results similar to Iliadi et al., supporting the notion that OA is required for
351 aversive learning in *Drosophila*.

352 Moreover, we found that OA release in the γ lobe of the MB plays a crucial role in
353 facilitating the release of DA via Oct β 1R, which is selectively coupled to increase
354 intracellular cyclic AMP levels by OA[76], in response to shock stimuli. This increased
355 release of DA drives a change in synaptic plasticity between KCs and the MBON and
356 promotes aversive learning[65, 67, 77-81]. The finding aligns with prior studies
357 showing that DANs are downstream of OANs in reward-based learning[20, 21, 82],
358 suggesting a conserved role for OA in mediating the DANs' ability to perceive US
359 signals in both positive and negative learning scenarios. It is noteworthy that our study
360 utilized a DA sensor[47] to specifically detect the release of DA itself, providing a more
361 direct assessment of its potential effects on downstream neurons, rather than
362 measuring DAN activity[20, 21]. In addition to confirming the involvement of OA in
363 aversive learning, our study also provides novel insights into the underlying input and
364 output circuitry through which OA operates (see Fig. 6G), which potentially indicates
365 that the CS and the US are not entirely independent events within the learning context,
366 but rather, one might have an impact on the other.

367 Nevertheless, further studies are needed to obtain a more comprehensive
368 understanding of the mechanisms through which OA contributes to associative
369 learning. Notably, previous studies found that Oct β 1R, expressed in KCs, is involved
370 in aversive learning[25], which operates as a parallel circuit along with the well-known
371 DA-dDA1 (MB- γ)-MBON pathways[83]. Additionally, in the context of appetitive
372 learning, the α 1-like OA receptor OAMB has been shown to play a role in engaging
373 octopaminergic signaling in KCs[22]. These intriguing findings suggest that OA may

374 exert a direct effect on KCs to affect associative learning. Thus, further research is
375 needed in order to unravel the complex interactions and mechanisms by which OA
376 modulates associative learning.

377 **Neuromodulators interact in associative learning**

378 As the primary center of associative memory in *Drosophila*, the MB uses ACh as the
379 predominant excitatory neurotransmitter released from KCs[58]. However, the MB
380 also receives converging inputs from other neuromodulators such as OA, DA, 5-HT,
381 and GABA. The interactions between these neuromodulator systems, as well as with
382 ACh, are essential for controlling the brain's states and neuronal computations[56].
383 Here, we show that odor- or shock-evoked release of OA requires ACh release from
384 KCs, and in turn, increases DA release, thereby forming a positive feedback loop that
385 is required for learning. However, our imaging results showed that KC activity is both
386 necessary and sufficient for OA release in the γ lobe of the MB, thereby influencing DA
387 release. We did not rule out the possibility that other inputs to OANs, as illustrated in
388 Fig. S3 where neurons of other classes, aside from KCs, form synaptic connections
389 with OANs, might contribute to DA release. This possibility opens up an intriguing
390 avenue for future research to explore the functional implications of these connections.
391 Additionally, recent research has shown that normal DAN synaptic release during
392 learning requires KC input to DAN[84]. In addition, KCs have been shown to activate
393 GABAergic APL neurons[85] and serotonergic dorsal paired medial (DPM)
394 neurons[64], both of which provide negative feedback to KCs. GABA release from
395 APL neurons is believed to contribute to odor-specific memory through sparse
396 coding[86], while 5-HT release from DPM neurons regulates the coincidence time
397 window of associative learning[64]. Thus, as the predominant neuron type in the MB,
398 KCs not only associate CS and US signals but also regulate a variety of
399 neuromodulators to form local feedback loops. These local reentrant loops allow for
400 moment-by-moment updates of both external (i.e., environmental) and internal
401 information, allowing for the appropriate reconfiguration of the flow of information
402 between KCs and MBONs, thus providing behavioral flexibility and the appropriate
403 responses to change the internal and external states of the organism[87].

404 The interplay between neuromodulators is both complex and essential for shaping the
405 activity of synaptic circuit elements to drive cognitive processes in both invertebrates
406 and mammals. In this respect, our study provides new insights by highlighting the
407 conserved interaction between OA and DA in invertebrates, offering a valuable
408 framework for understanding the complex interplay between DA and other
409 neurotransmitters in associative learning processes. Additionally, a recent study in

410 mammals showed that continuous interactions and updating between ACh and DA
411 signaling in the nucleus accumbens are critical for regulating the striatal output that
412 underlies the acquisition of Pavlovian learning of reward-predicting cues[88, 89].
413 Given the similarities between OA-DA interaction in invertebrates and the ACh-DA
414 interaction in mammals, it is reasonable to speculate that such interactions are a
415 fundamental feature of the central nervous system. The discovery that such
416 conserved interactions exist between distinct neuromodulator systems provides
417 valuable new insights into the mechanisms that underlie cognitive processes and may
418 have important implications with respect to developing new therapies for cognitive
419 disorders.

420 **METHODS**

421 Detailed methods are provided in the online version of this paper and include the
422 following:

423 KEY RESOURCES TABLE

424 EXPERIMENTAL MODEL AND SUBJECT DETAILS

425 ● Cell lines

426 ● Flies

427 DETAILED METHODS

428 ● Molecular biology

429 ● Expression of GRAB_{OA} sensors in cultured cells

430 ● Fluorescence imaging of cultured cells

431 ● Tango assay

432 ● RFlamp cAMP measuring assay

433 ● Spectra measurements

434 ● Fast-scan cyclic voltammetry

435 ● Two-photon *in vivo* imaging of flies

436 ● Behavioral assay

437 QUANTIFICATION AND STATISTICAL ANALYSIS

438 ● Imaging experiments

439 ● Behavioral experiments

440 ● Statistical analysis

441

442 **ACKNOWLEDGMENTS**

443 We thank Yi Rao for providing access to the two-photon microscope. We thank Yi
444 Zhong, Lianzhang Wang and Bohan Zhao for helping with T-maze assay. We thank
445 Jun Chu for providing RFlamp sensor. We thank the imaging core facility of State Key
446 Laboratory of Membrane Biology at Peking University (Ye Liang). We thank the Core
447 Facility of Drosophila Resource and Technology of CAS Center for Excellence in
448 Molecular Cell Science (Wei Wu). We thank the National Center for Protein Sciences
449 at Peking University for support and assistance with the Opera Phenix high content
450 screening system. We thank Seth Tomchik, Stephen Zhang, Andrew Lin, Yan Li,
451 Emmanuel Perisse, and Woo Jae Kim for valuable feedback regarding the manuscript.
452 Finally, we thank Yulin Zhao, Hui Dong, Bin Luo and other Li lab members for helpful
453 suggestions and comments on the manuscript.

454 **FUNDING**

455 This work was supported by grants to Yulong Li from the National Key R&D Program
456 of China (2019YFE011781), the National Natural Science Foundation of China
457 (31925017 and 31871087), the NIH BRAIN Initiative (1U01NS113358 and
458 1U01NS120824), the Feng Foundation of Biomedical Research, the Clement and
459 Xinxin Foundation, the Peking-Tsinghua Center for Life Sciences, the State Key
460 Laboratory of Membrane Biology at Peking University School of Life Sciences, and
461 the New Cornerstone Science Foundation through the New Cornerstone Investigator
462 Program and the XPLOER PRIZE.

463 **AUTHOR CONTRIBUTIONS**

464 Y.L. supervised the project. M.L. performed all imaging and behavioral experiments
465 (except as otherwise noted). R.Z. and M.L. analyzed EM data. R.C. and H.W.
466 performed the experiments related to sensor development, optimization and
467 characterization in cultured cells. Y.X. performed FSCV experiments. Y.L. and M.L.
468 wrote the manuscript with input from all other authors.

469

470

471 **DECLARATION OF INTEREST**

472 The authors declare no competing interests. Y.L. is a member of the journal's advisory
473 board.

474 **REFERENCES**

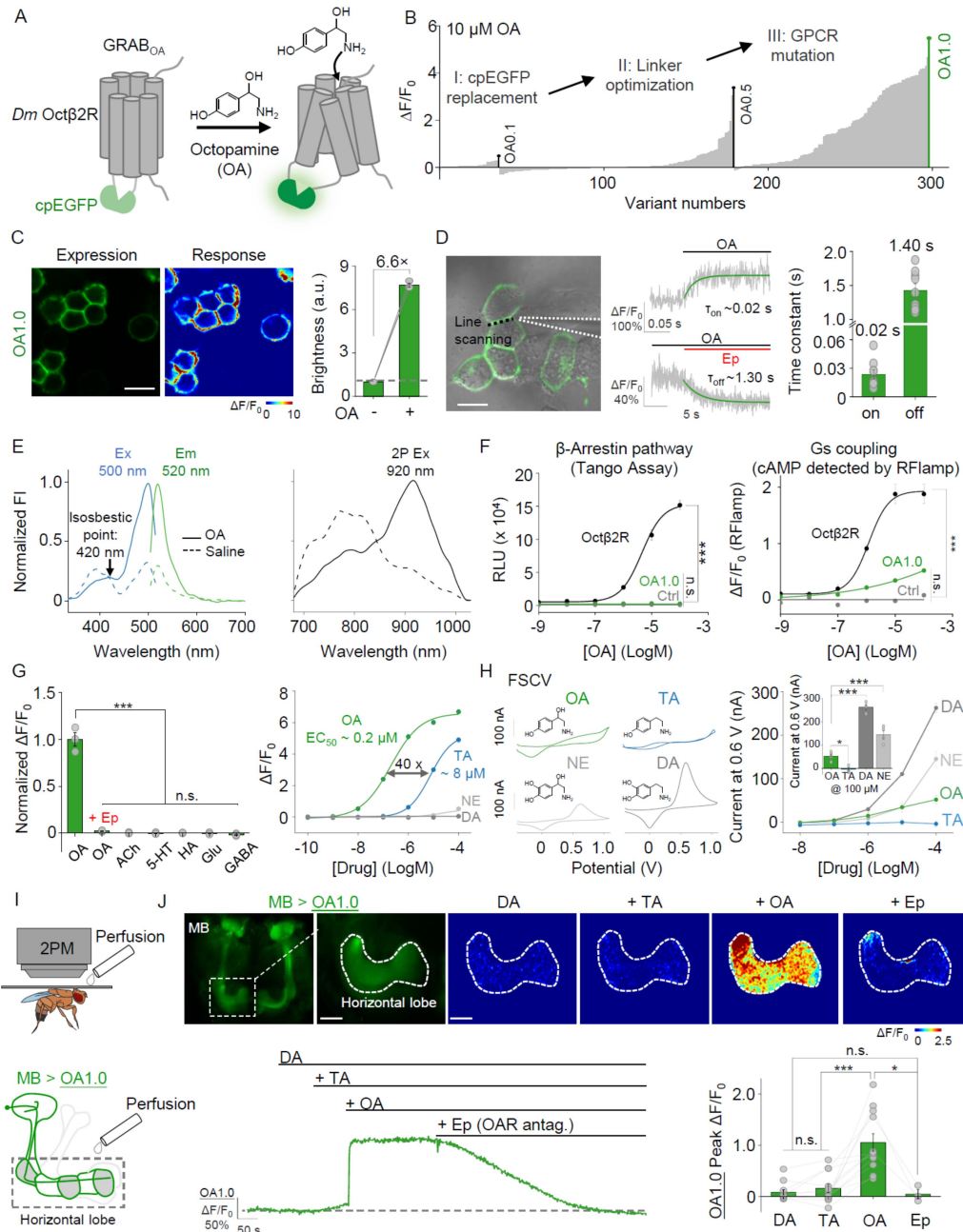
- 475 1. Roeder, T., *Octopamine in invertebrates*. Prog Neurobiol, 1999. **59**(5): p. 533-61.
- 476 2. Roeder, T., *Tyramine and octopamine: ruling behavior and metabolism*. Annu Rev
477 Entomol, 2005. **50**: p. 447-77.
- 478 3. Axelrod, J. and J.M. Saavedra, *Octopamine*. Nature, 1977. **265**(5594): p. 501-4.
- 479 4. Sandler, M., et al., *Deficient production of tyramine and octopamine in cases of*
480 *depression*. Nature, 1979. **278**(5702): p. 357-358.
- 481 5. Berry, M.D., *Mammalian central nervous system trace amines. Pharmacologic*
482 *amphetamines, physiologic neuromodulators*. J Neurochem, 2004. **90**(2): p. 257-71.
- 483 6. Crocker, A. and A. Sehgal, *Octopamine regulates sleep in drosophila through protein*
484 *kinase A-dependent mechanisms*. J Neurosci, 2008. **28**(38): p. 9377-85.
- 485 7. Zhou, C., Y. Rao, and Y. Rao, *A subset of octopaminergic neurons are important for*
486 *Drosophila aggression*. Nat Neurosci, 2008. **11**(9): p. 1059-67.
- 487 8. Lee, H.G., et al., *Octopamine receptor OAMB is required for ovulation in Drosophila*
488 *melanogaster*. Dev Biol, 2003. **264**(1): p. 179-90.
- 489 9. Monastirioti, M., *Distinct octopamine cell population residing in the CNS abdominal*
490 *ganglion controls ovulation in Drosophila melanogaster*. Dev Biol, 2003. **264**(1): p.
491 38-49.
- 492 10. Goosey, M.W. and D.J. Candy, *Effects of d- and l-octopamine and of pharmacological*
493 *agents on the metabolism of locust flight muscle*. Biochemical Society Transactions,
494 1980. **8**(5): p. 532-533.
- 495 11. Orchard, I., J.M. Ramirez, and A.B. Lange, *A Multifunctional Role for Octopamine in*
496 *Locust Flight*. Annual Review of Entomology, 1993. **38**(1): p. 227-249.
- 497 12. Suver, M.P., A. Mamiya, and M.H. Dickinson, *Octopamine neurons mediate*
498 *flight-induced modulation of visual processing in Drosophila*. Curr Biol, 2012. **22**(24): p.
499 2294-302.
- 500 13. van Breugel, F., M.P. Suver, and M.H. Dickinson, *Octopaminergic modulation of the*
501 *visual flight speed regulator of Drosophila*. J Exp Biol, 2014. **217**(Pt 10): p. 1737-44.
- 502 14. Lim, J., et al., *The octopamine receptor Oct β 2R regulates ovulation in Drosophila*
503 *melanogaster*. PLoS One, 2014. **9**(8): p. e104441.
- 504 15. Li, Y., et al., *Octopamine controls starvation resistance, life span and metabolic traits*
505 *in Drosophila*. Sci Rep, 2016. **6**: p. 35359.
- 506 16. Hoyer, S.C., et al., *Octopamine in male aggression of Drosophila*. Curr Biol, 2008.
507 **18**(3): p. 159-67.
- 508 17. Stevenson, P.A., et al., *Octopamine and experience-dependent modulation of*
509 *aggression in crickets*. J Neurosci, 2005. **25**(6): p. 1431-41.
- 510 18. Andrews, J.C., et al., *Octopamine neuromodulation regulates Gr32a-linked*

- 511 aggression and courtship pathways in *Drosophila* males. PLoS Genet, 2014. **10**(5): p.
512 e1004356.
- 513 19. Schwaerzel, M., et al., *Dopamine and Octopamine Differentiate between Aversive and*
514 *Appetitive Olfactory Memories in Drosophila*. J Neurosci, 2003. **23**(33): p. 10495-502.
- 515 20. Burke, C.J., et al., *Layered reward signalling through octopamine and dopamine in*
516 *Drosophila*. Nature, 2012. **492**(7429): p. 433-7.
- 517 21. Liu, C., et al., *A subset of dopamine neurons signals reward for odour memory in*
518 *Drosophila*. Nature, 2012. **488**(7412): p. 512-6.
- 519 22. Kim, Y.C., et al., *Appetitive learning requires the alpha1-like octopamine receptor*
520 *OAMB in the Drosophila mushroom body neurons*. J Neurosci, 2013. **33**(4): p. 1672-7.
- 521 23. Wu, C.L., et al., *An octopamine-mushroom body circuit modulates the formation of*
522 *anesthesia-resistant memory in Drosophila*. Curr Biol, 2013. **23**(23): p. 2346-54.
- 523 24. Sayin, S., et al., *A Neural Circuit Arbitrates between Persistence and Withdrawal in*
524 *Hungry Drosophila*. Neuron, 2019. **104**(3): p. 544-558 e6.
- 525 25. Sabandal, J.M., et al., *Concerted Actions of Octopamine and Dopamine Receptors*
526 *Drive Olfactory Learning*. J Neurosci, 2020. **40**(21): p. 4240-4250.
- 527 26. Hermanns, T., et al., *Octopamine mediates sugar relief from a chronic-stress-induced*
528 *depression-like state in Drosophila*. Curr Biol, 2022. **32**(18): p. 4048-4056 e3.
- 529 27. Monastirioti, M., C.E. Linn, Jr., and K. White, *Characterization of Drosophila tyramine*
530 *beta-hydroxylase gene and isolation of mutant flies lacking octopamine*. J Neurosci,
531 1996. **16**(12): p. 3900-11.
- 532 28. Yarali, A. and B. Gerber, *A Neurogenetic Dissociation between Punishment-, Reward-,*
533 *and Relief-Learning in Drosophila*. Front Behav Neurosci, 2010. **4**: p. 189.
- 534 29. Iliadi, K.G., N. Iliadi, and G.L. Boulianne, *Drosophila mutants lacking octopamine*
535 *exhibit impairment in aversive olfactory associative learning*. Eur J Neurosci, 2017.
536 **46**(5): p. 2080-2087.
- 537 30. Heisenberg, M., et al., *Drosophila mushroom body mutants are deficient in olfactory*
538 *learning*. J Neurogenet, 1985. **2**(1): p. 1-30.
- 539 31. de Belle, J.S. and M. Heisenberg, *Associative odor learning in Drosophila abolished*
540 *by chemical ablation of mushroom bodies*. Science, 1994. **263**(5147): p. 692-5.
- 541 32. McGuire, S.E., P.T. Le, and R.L. Davis, *The role of Drosophila mushroom body*
542 *signaling in olfactory memory*. Science, 2001. **293**(5533): p. 1330-3.
- 543 33. Dubnau, J., et al., *Disruption of neurotransmission in Drosophila mushroom body*
544 *blocks retrieval but not acquisition of memory*. Nature, 2001. **411**(6836): p. 476-480.
- 545 34. Tanaka, N.K., H. Tanimoto, and K. Ito, *Neuronal assemblies of the Drosophila*
546 *mushroom body*. J Comp Neurol, 2008. **508**(5): p. 711-55.
- 547 35. Butcher, N.J., et al., *Different classes of input and output neurons reveal new features*
548 *in microglomeruli of the adult Drosophila mushroom body calyx*. J Comp Neurol, 2012.
549 **520**(10): p. 2185-201.
- 550 36. Aso, Y., et al., *The mushroom body of adult Drosophila characterized by GAL4 drivers*.
551 J Neurogenet, 2009. **23**(1-2): p. 156-72.
- 552 37. Ikemoto, Y., S. Kawai, and J. Mizutani, *Microdialysis for the Analysis of Insect*
553 *Haemolymph*. Bioscience, Biotechnology, and Biochemistry, 1993. **57**(3): p. 402-404.
- 554 38. Bendahan, G., M.L. Boatell, and N. Mahy, *Decreased cortical octopamine level in*

- 555 *basal forebrain lesioned rats: a microdialysis study*. *Neurosci Lett*, 1993. **152**(1-2): p.
556 45-7.
- 557 39. Fang, H., T.L. Vickrey, and B.J. Venton, *Analysis of biogenic amines in a single*
558 *Drosophila larva brain by capillary electrophoresis with fast-scan cyclic voltammetry*
559 *detection*. *Anal Chem*, 2011. **83**(6): p. 2258-64.
- 560 40. Cooper, S.E. and B.J. Venton, *Fast-scan cyclic voltammetry for the detection of*
561 *tyramine and octopamine*. *Anal Bioanal Chem*, 2009. **394**(1): p. 329-36.
- 562 41. Pyakurel, P., E. Privman Champaloux, and B.J. Venton, *Fast-Scan Cyclic Voltammetry*
563 *(FSCV) Detection of Endogenous Octopamine in Drosophila melanogaster Ventral*
564 *Nerve Cord*. *ACS Chem Neurosci*, 2016. **7**(8): p. 1112-9.
- 565 42. Jing, M., et al., *A genetically encoded fluorescent acetylcholine indicator for in vitro*
566 *and in vivo studies*. *Nat Biotechnol*, 2018. **36**(8): p. 726-737.
- 567 43. Sun, F., et al., *A Genetically Encoded Fluorescent Sensor Enables Rapid and Specific*
568 *Detection of Dopamine in Flies, Fish, and Mice*. *Cell*, 2018. **174**(2): p. 481-496 e19.
- 569 44. Feng, J., et al., *A Genetically Encoded Fluorescent Sensor for Rapid and Specific In*
570 *Vivo Detection of Norepinephrine*. *Neuron*, 2019. **102**(4): p. 745-761 e8.
- 571 45. Jing, M., et al., *An optimized acetylcholine sensor for monitoring in vivo cholinergic*
572 *activity*. *Nat Methods*, 2020. **17**(11): p. 1139-1146.
- 573 46. Peng, W., et al., *Regulation of sleep homeostasis mediator adenosine by basal*
574 *forebrain glutamatergic neurons*. *Science*, 2020. **369**(6508).
- 575 47. Sun, F., et al., *Next-generation GRAB sensors for monitoring dopaminergic activity in*
576 *vivo*. *Nat Methods*, 2020. **17**(11): p. 1156-1166.
- 577 48. Dong, A., et al., *A fluorescent sensor for spatiotemporally resolved imaging of*
578 *endocannabinoid dynamics in vivo*. *Nat Biotechnol*, 2021.
- 579 49. Wan, J., et al., *A genetically encoded sensor for measuring serotonin dynamics*. *Nat*
580 *Neurosci*, 2021. **24**(5): p. 746-752.
- 581 50. Wu, Z., et al., *A sensitive GRAB sensor for detecting extracellular ATP in vitro and in*
582 *vivo*. *Neuron*, 2022. **110**(5): p. 770-782 e5.
- 583 51. Dong, H., et al., *Genetically encoded sensors for measuring histamine release both*
584 *in vitro and in vivo*. *Neuron*, 2023.
- 585 52. Wu, Z., et al., *Neuronal activity-induced, equilibrative nucleoside*
586 *transporter-dependent, somatodendritic adenosine release revealed by a GRAB*
587 *sensor*. *Proc Natl Acad Sci U S A*, 2023. **120**(14): p. e2212387120.
- 588 53. Jing, M., et al., *G-protein-coupled receptor-based sensors for imaging neurochemicals*
589 *with high sensitivity and specificity*. *J Neurochem*, 2019. **151**(3): p. 279-288.
- 590 54. Barnea, G., et al., *The genetic design of signaling cascades to record receptor*
591 *activation*. *Proc Natl Acad Sci U S A*, 2008. **105**(1): p. 64-9.
- 592 55. Busch, S., et al., *A map of octopaminergic neurons in the Drosophila brain*. *J Comp*
593 *Neurol*, 2009. **513**(6): p. 643-67.
- 594 56. Li, F., et al., *The connectome of the adult Drosophila mushroom body provides*
595 *insights into function*. *Elife*, 2020. **9**.
- 596 57. Scheffer, L.K., et al., *A connectome and analysis of the adult Drosophila central brain*.
597 *Elife*, 2020. **9**.
- 598 58. Barnstedt, O., et al., *Memory-Relevant Mushroom Body Output Synapses Are*

- 599 *Cholinergic*. *Neuron*, 2016. **89**(6): p. 1237-1247.
- 600 59. Tadres, D., et al., *An essential experimental control for functional connectivity mapping*
601 *with optogenetics*. *bioRxiv*, 2022: p. 2022.05.26.493610.
- 602 60. Armbruster, B.N., et al., *Evolving the lock to fit the key to create a family of G*
603 *protein-coupled receptors potentially activated by an inert ligand*. *Proc Natl Acad Sci U S*
604 *A*, 2007. **104**(12): p. 5163-8.
- 605 61. Becnel, J., et al., *DREADDs in Drosophila: a pharmacogenetic approach for*
606 *controlling behavior, neuronal signaling, and physiology in the fly*. *Cell Rep*, 2013. **4**(5):
607 p. 1049-59.
- 608 62. Roth, B.L., *DREADDs for Neuroscientists*. *Neuron*, 2016. **89**(4): p. 683-94.
- 609 63. Nagai, Y., et al., *Deschloroclozapine, a potent and selective chemogenetic actuator*
610 *enables rapid neuronal and behavioral modulations in mice and monkeys*. *Nat*
611 *Neurosci*, 2020. **23**(9): p. 1157-1167.
- 612 64. Zeng, J., et al., *Local 5-HT signaling bi-directionally regulates the coincidence time*
613 *window for associative learning*. *Neuron*, 2023.
- 614 65. Hige, T., et al., *Heterosynaptic Plasticity Underlies Aversive Olfactory Learning in*
615 *Drosophila*. *Neuron*, 2015. **88**(5): p. 985-998.
- 616 66. Felsenberg, J., et al., *Integration of Parallel Opposing Memories Underlies Memory*
617 *Extinction*. *Cell*, 2018. **175**(3): p. 709-722.e15.
- 618 67. Perisse, E., et al., *Aversive Learning and Appetitive Motivation Toggle Feed-Forward*
619 *Inhibition in the Drosophila Mushroom Body*. *Neuron*, 2016. **90**(5): p. 1086-99.
- 620 68. Stahl, A., et al., *Associative learning drives longitudinally graded presynaptic plasticity*
621 *of neurotransmitter release along axonal compartments*. *Elife*, 2022. **11**.
- 622 69. Aso, Y., et al., *Mushroom body output neurons encode valence and guide*
623 *memory-based action selection in Drosophila*. *Elife*, 2014. **3**: p. e04580.
- 624 70. Davis, R.L., *SnapShot: Olfactory Classical Conditioning of Drosophila*. *Cell*, 2015.
625 **163**(2): p. 524-524 e1.
- 626 71. Dedic, N., et al., *Therapeutic Potential of TAAR1 Agonists in Schizophrenia: Evidence*
627 *from Preclinical Models and Clinical Studies*. *International Journal of Molecular*
628 *Sciences*, 2021. **22**(24).
- 629 72. Halff, E.F., et al., *Trace amine-associated receptor 1 (TAAR1) agonism as a new*
630 *treatment strategy for schizophrenia and related disorders*. *Trends Neurosci*, 2023.
631 **46**(1): p. 60-74.
- 632 73. Borowsky, B., et al., *Trace amines: identification of a family of mammalian G*
633 *protein-coupled receptors*. *Proc Natl Acad Sci U S A*, 2001. **98**(16): p. 8966-71.
- 634 74. Farooqui, T., et al., *Modulation of Early Olfactory Processing by an Octopaminergic*
635 *Reinforcement Pathway in the Honeybee*. *The Journal of Neuroscience*, 2003. **23**: p.
636 5370 - 5380.
- 637 75. Mizunami, M. and Y. Matsumoto, *Roles of Octopamine and Dopamine Neurons for*
638 *Mediating Appetitive and Aversive Signals in Pavlovian Conditioning in Crickets*.
639 *Frontiers in Physiology*, 2017. **8**.
- 640 76. Maqueira, B., H. Chatwin, and P.D. Evans, *Identification and characterization of a*
641 *novel family of Drosophila beta-adrenergic-like octopamine G-protein coupled*
642 *receptors*. *J Neurochem*, 2005. **94**(2): p. 547-60.

- 643 77. Cohn, R., I. Morante, and V. Ruta, *Coordinated and Compartmentalized*
644 *Neuromodulation Shapes Sensory Processing in Drosophila*. Cell, 2015. **163**(7): p.
645 1742-55.
- 646 78. Waddell, S., *Reinforcement signalling in Drosophila; dopamine does it all after all*. Curr
647 Opin Neurobiol, 2013. **23**(3): p. 324-9.
- 648 79. Oswald, D., et al., *Activity of Defined Mushroom Body Output Neurons Underlies*
649 *Learned Olfactory Behavior in Drosophila*. Neuron, 2015. **86**(2): p. 417-427.
- 650 80. Aso, Y., et al., *Three dopamine pathways induce aversive odor memories with*
651 *different stability*. PLoS Genet, 2012. **8**(7): p. e1002768.
- 652 81. Aso, Y. and G.M. Rubin, *Dopaminergic neurons write and update memories with*
653 *cell-type-specific rules*. Elife, 2016. **5**.
- 654 82. Huetteroth, W., et al., *Sweet taste and nutrient value subdivide rewarding*
655 *dopaminergic neurons in Drosophila*. Curr Biol, 2015. **25**(6): p. 751-758.
- 656 83. Kim, Y.C., H.G. Lee, and K.A. Han, *D1 dopamine receptor dDA1 is required in the*
657 *mushroom body neurons for aversive and appetitive learning in Drosophila*. J
658 Neurosci, 2007. **27**(29): p. 7640-7.
- 659 84. Cervantes-Sandoval, I., et al., *Reciprocal synapses between mushroom body and*
660 *dopamine neurons form a positive feedback loop required for learning*. Elife, 2017. **6**.
- 661 85. Liu, X. and R.L. Davis, *The GABAergic anterior paired lateral neuron suppresses and*
662 *is suppressed by olfactory learning*. Nat Neurosci, 2009. **12**(1): p. 53-9.
- 663 86. Lin, A.C., et al., *Sparse, decorrelated odor coding in the mushroom body enhances*
664 *learned odor discrimination*. Nat Neurosci, 2014. **17**(4): p. 559-68.
- 665 87. Person, A.L. and K. Khodakhah, *Recurrent Feedback Loops in Associative Learning*.
666 Neuron, 2016. **89**(3): p. 427-30.
- 667 88. Skirzewski, M., et al., *Continuous cholinergic-dopaminergic updating in the nucleus*
668 *accumbens underlies approaches to reward-predicting cues*. Nat Commun, 2022.
669 **13**(1): p. 7924.
- 670 89. Krok, A.C., et al., *Intrinsic dopamine and acetylcholine dynamics in the striatum of*
671 *mice*. Nature, 2023.
- 672



674

675 **Figure 1. Development and characterization of the GRAB_{OA1.0} (OA1.0) sensor in**
 676 **HEK293T cells and living flies.**

677 (A) Schematic illustration depicting the strategy for developing the GRAB_{OA} sensor. Ligand
 678 binding activates the sensor, inducing a change in EGFP fluorescence.

679 (B) Screening and optimization steps of GRAB_{OA} sensors, and the resulting change in
 680 fluorescence ($\Delta F/F_0$) in response to 10 μM OA.

681 (C) Expression, fluorescence change in response to 100 μ M OA, and summary data measured
682 in HEK293T cells expressing OA1.0; n = 3 wells containing >500 cells each.

683 (D) τ_{on} and τ_{off} were measured in OA1.0-expressing cells in response to OA and epinastine
684 (Ep), respectively, in line-scan mode; an example image (left), representative traces (middle),
685 and summary data (right) are shown; n \geq 9 cells from 3 cultures; the dotted black line in the
686 image indicates the line-scanning region.

687 (E) One-photon (1P) excitation (ex) and emission (em) spectra (left) and two-photon (2P)
688 excitation spectra (right) of OA1.0 were measured in the absence and presence of OA; FI,
689 fluorescence intensity.

690 (F) Left: The Tango assay was used to measure β -arrestin-mediated signaling in cells
691 expressing OA1.0 or wild-type (WT) Oct β 2R and treated with increasing concentrations of OA;
692 n = 3 wells containing >1000 cells each. Right: The RFlamp assay was used to measure Gs
693 coupling in cells expressing OA1.0 or Oct β 2R; n = 3 wells containing >30 cells each.

694 (G) Left: Normalized change in fluorescence measured in OA1.0-expressing cells in response
695 to the indicated compounds applied at 10 μ M (except Ep, which was applied at 100 μ M); n = 3
696 wells containing >300 cells each. Right: Dose-response curves measured in
697 OA1.0-expressing cells in response to OA, tyramine (TA), dopamine (DA), and norepinephrine
698 (NE), with the corresponding EC₅₀ values shown; n = 3 wells containing >300 cells each. ACh,
699 acetylcholine; Glu, glutamate; GABA, γ -aminobutyric acid.

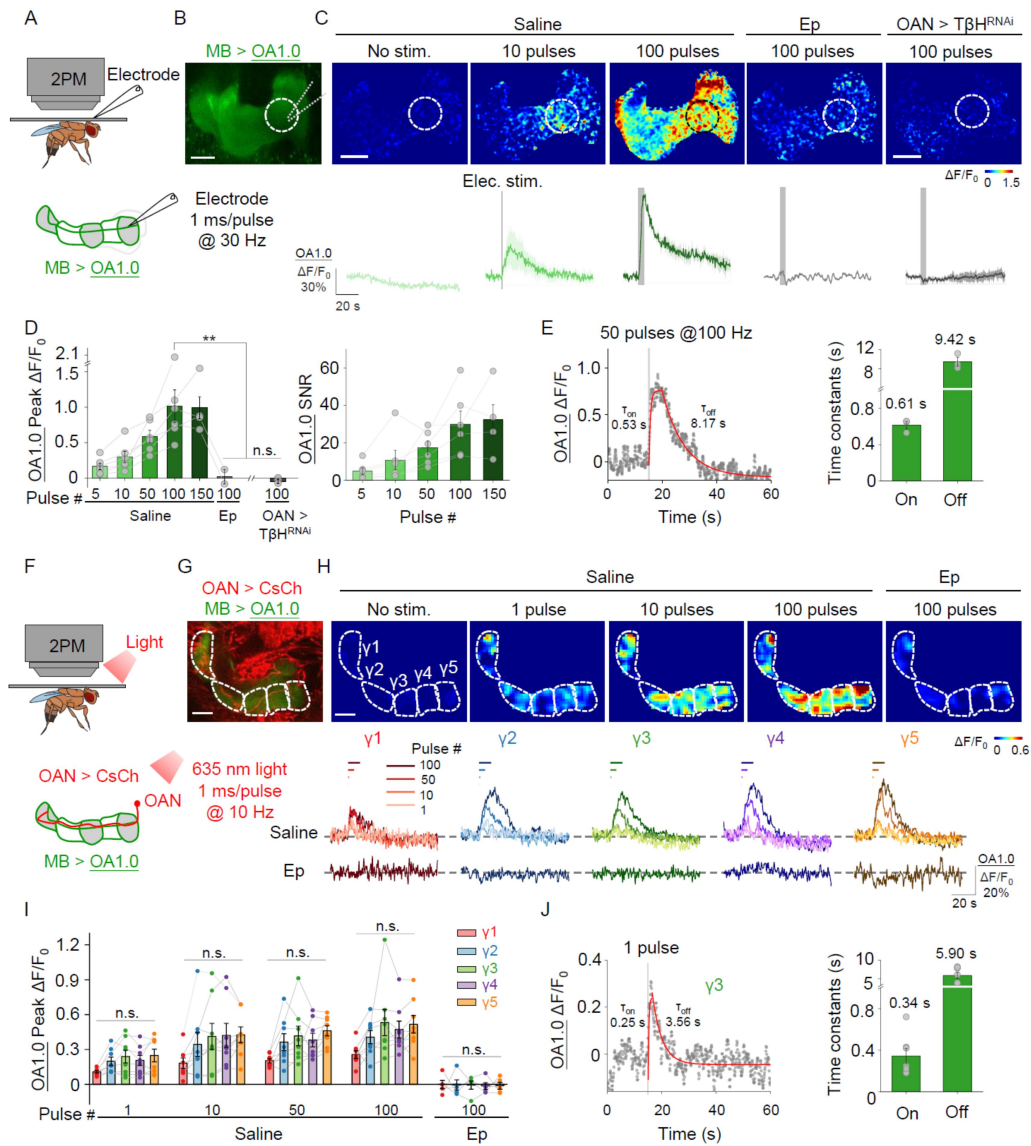
700 (H) Left: Exemplar cyclic voltammograms for 100 μ M OA, TA, DA, and NE measured using
701 fast-scan cyclic voltammetry (FSCV); the traces were averaged from separate trials. Right:
702 The voltammetric current responses at 0.6 V were measured in accordance with the
703 increasing concentrations of OA, TA, DA, and NE; the inset shows the summary data in
704 response to 100 μ M OA, TA, DA, and NE.

705 (I) Schematic illustration depicting the *in vivo* imaging setup using and perfusion to the brain of
706 flies expressing OA1.0 in the mushroom body (MB, 30y-GAL4-driven).

707 (J) Representative *in vivo* fluorescence images (top left), pseudocolor images (top right),
708 traces (bottom left), and summary (bottom right) of the change in OA1.0 fluorescence
709 measured in the MB horizontal lobe in response to application of DA (500 μ M), TA (500 μ M),
710 OA (500 μ M), and Ep (100 μ M).

711 In this and subsequent Fig.s, all summary data are presented as the mean \pm SEM,
712 superimposed with individual data.

713 *p < 0.05, ***p < 0.001, and n.s., not significant (for F, G, and H, one-way ANOVA with Tukey's
714 post hoc test; for J, paired or unpaired Student's t-test). Scale bar = 20 μ m.



716

717

Figure 2. OA1.0 can report the release of OA release *in vivo*.

718

(A) Schematic illustration depicting the experimental setup in which a transgenic fly expressing OA1.0 in the MB (MB247-LexA-driven) is fixed under a two-photon microscope (2PM) and a glass electrode is used to apply electrical stimuli near the MB.

719

(B) Example fluorescence image of OA1.0 expressed in the MB. The dotted circle represents the region of interest (ROI) used for subsequent analysis.

720

(C) Representative pseudocolor images (top) and corresponding traces (bottom) of the change in OA1.0 fluorescence in response to the indicated number of electrical stimuli in a control fly, a control fly treated with 100 μ M epinastine (Ep), and an OAN (Tdc2-GAL4-driven) > T β H^{RNAi} fly.

721

(D) OA1.0 Peak $\Delta F/F_0$ vs Pulse # for Saline and Ep. ** indicates statistical significance.

722

(E) OA1.0 SNR vs Pulse # for Saline and Ep. n.s. indicates not significant.

723

(F) Schematic of light stimulation setup.

724

(G) OA1.0 $\Delta F/F_0$ traces for OAN > CsCh MB > OA1.0 under various stimulation conditions. Time constants (s) for On and Off phases are shown.

725

(H) OA1.0 Peak $\Delta F/F_0$ vs Pulse # for Saline and Ep across y1-y5 neurons. n.s. indicates not significant.

726

(I) OA1.0 SNR vs Pulse # for Saline and Ep across y1-y5 neurons. n.s. indicates not significant.

(J) Time constants (s) for On and Off phases for a single pulse in y3 neurons.

727 (D) Summary of peak $\Delta F/F_0$ (left) and the signal-to-noise ratio (SNR, right) measured in
728 response to electrical stimuli for the indicated conditions; n = 2-6 flies/group.

729 (E) Left: Time course of $\Delta F/F_0$ measured in OA1.0-expressing flies in response to 50 electrical
730 stimuli applied at 100 Hz; the rise and decay phases were fitted with a single-exponential
731 function (red traces). Right: Summary of τ_{on} and τ_{off} ; n = 3 flies/group.

732 (F) Schematic illustration depicting the experimental setup for optogenetic stimulation.

733 (G) Example dual-color fluorescence image of OA1.0 expressed in the MB (green,
734 MB247-LexA-driven) and CsChrimson-mCherry expressed in OANs (red, Tdc2-GAL4-driven);
735 the $\Delta F/F_0$). The $\gamma 1$ - $\gamma 5$ compartments of the MB are indicated using dashed lines.

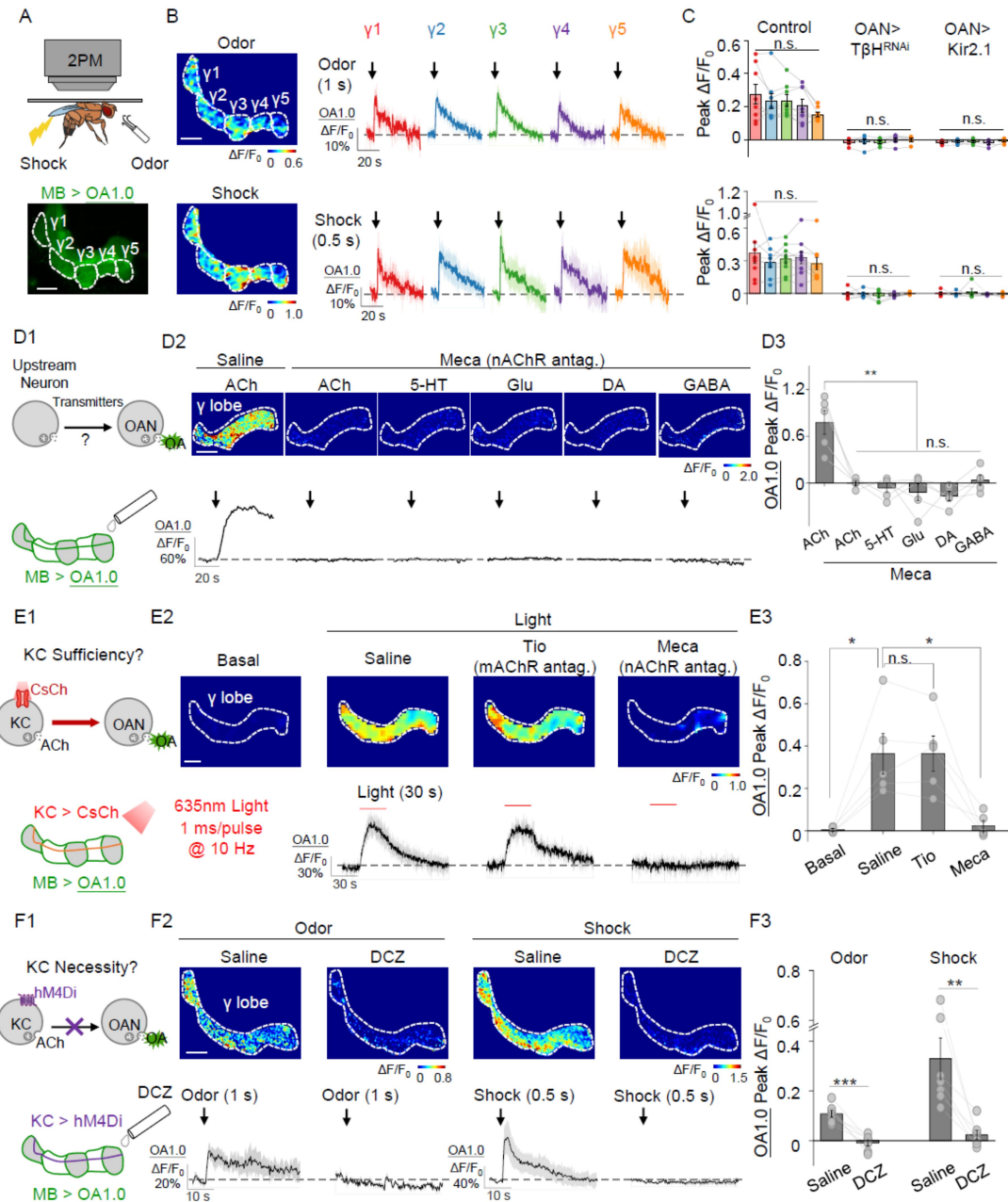
736 (H) Representative pseudocolor images (top) and corresponding traces (bottom) of the
737 change in OA1.0 fluorescence measured in response to the indicated number of optogenetic
738 stimuli applied either in saline or 100 μ M Ep.

739 (I) Summary of peak $\Delta F/F_0$ measured in response to optogenetic stimuli; n = 8 flies/group.

740 (J) Left: Time course of $\Delta F/F_0$ measured in the $\gamma 3$ compartment in response to a single laser
741 pulse; the rise and decay phases were fitted with a single-exponential function (red traces).
742 Right: Summary of τ_{on} and τ_{off} ; n = 7 flies/group.

743 **p < 0.01, and n.s., not significant (for D, paired or unpaired Student's t-test; for I, one-way
744 ANOVA with Tukey's post hoc test). Scale bar = 20 μ m.

ORIGINAL UNEDITED MANUSCRIPT



746

747 **Figure 3. OA1.0 reveals that OA release induced by odor and shock stimuli is activated**
 748 **by ACh released from KCs.**

749 (A) Schematic diagram depicting the experimental setup for 2PM with odor and body shock
 750 stimulation in flies expressing OA1.0 in the MB (MB247-LexA-driven), with an example
 751 fluorescent image of the MB shown below.

752 (B-C) Representative pseudocolor images (B, left), traces (B, right), and summary (C) of the

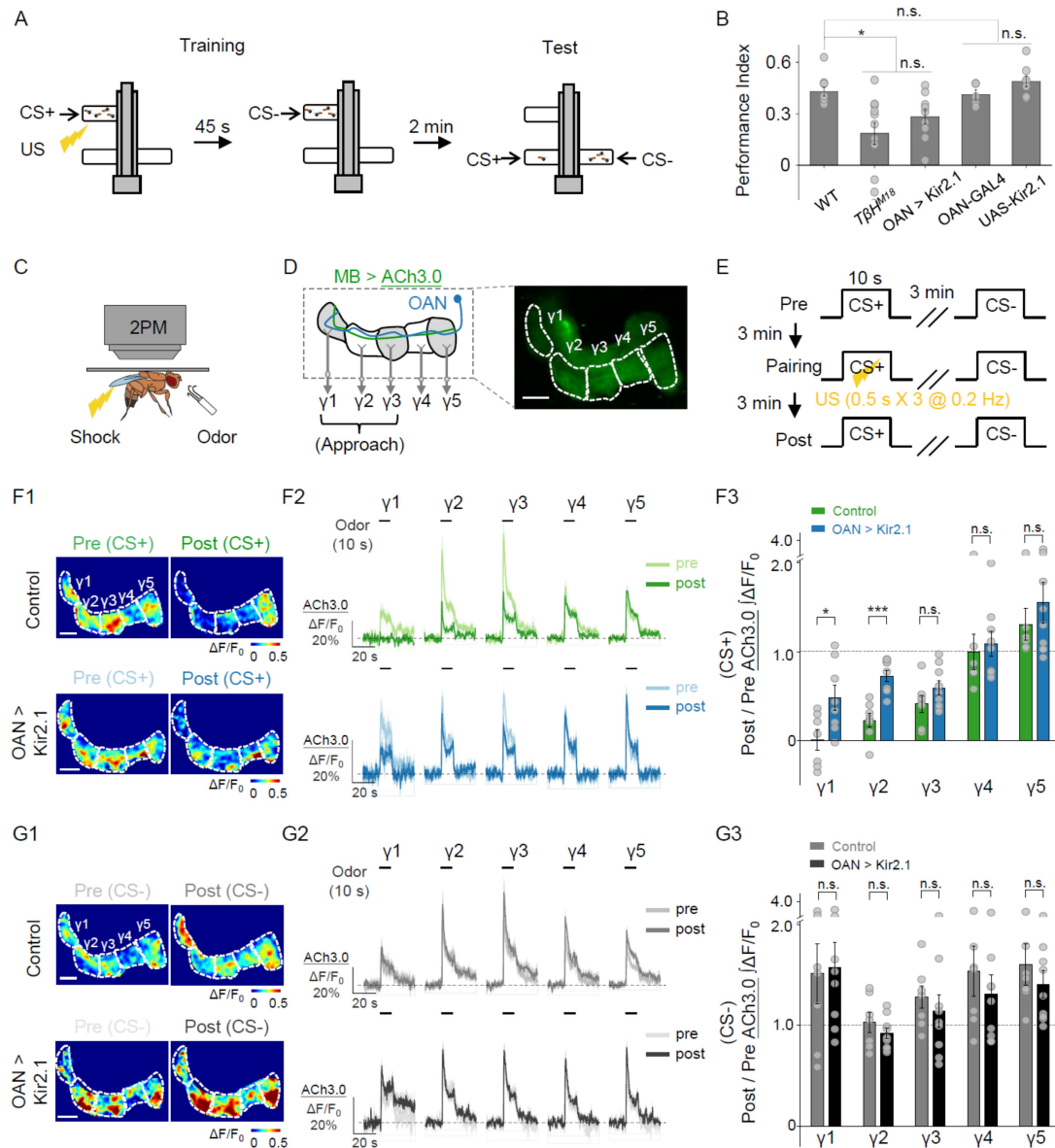
753 change in OA1.0 fluorescence measured in response to odorant application (top) and body
754 shock (bottom) in OA1.0-expressing flies (n = 8-9) and OA1.0-expressing flies co-expressing
755 $T\beta H^{RNAi}$ (n = 6) or Kir2.1 (n = 5) in OANs (Tdc2-GAL4-driven).

756 (D) Schematic diagram (D1) depicting the strategy used to apply compounds to the brain of
757 flies expressing OA1.0 in the MB (MB247-LexA-driven). Also shown are representative
758 pseudocolor images (D2, top), traces (D2, bottom), and summary (D3) of the change in OA1.0
759 fluorescence in response to the indicated compounds (1 mM each) applied in the absence or
760 presence of the nAChR antagonist Meca (100 μ M); n = 5 flies/group.

761 (E) Schematic diagram (E1) depicting the strategy in which CsChrimson expressed in KCs
762 (R13F02-GAL4-driven) was activated using optogenetic stimulation, and OA1.0 fluorescence
763 was measured in the MB (MB247-LexA-driven). Also shown are representative pseudocolor
764 images (E2, top), traces (E2, bottom), and summary (E3) of the change in OA1.0 fluorescence
765 in response to optogenetic stimulation in saline, the muscarinic ACh receptor antagonist Tio
766 (100 μ M), and Meca (100 μ M); n = 5 flies/group.

767 (F) Schematic diagram (F1) depicting the strategy in which hM4Di expressed in KCs
768 (30y-GAL4-driven) was silenced by applying 30 nM deschloroclozapine (DCZ), and OA1.0
769 fluorescence was measured in the MB. Also shown are representative pseudocolor images
770 (F2, top), traces (F2, bottom), and summary (F3) of the change in OA1.0 fluorescence in
771 response to odor or electrical body shock in the absence or presence of 30 nM DCZ; n = 7
772 flies/group.

773 *p < 0.05, **p < 0.01, ***p < 0.001, and n.s., not significant (for C, one-way ANOVA with
774 Tukey's post hoc test; for D3-F3, paired Student's t-test). Scale bar = 20 μ m.



776

777 **Figure 4. OA plays an essential role in aversive learning and synaptic plasticity in KCs**
 778 **in the MB.**

779 (A) Schematic diagram depicting the T-maze protocol for measuring aversive learning in
 780 *Drosophila*.

781 (B) Summary of the performance index measured in WT flies and the indicated transgenic flies.

782 OAN-GAL4 and UAS-Kir2.1 served as control groups; n=5-10 for each group.

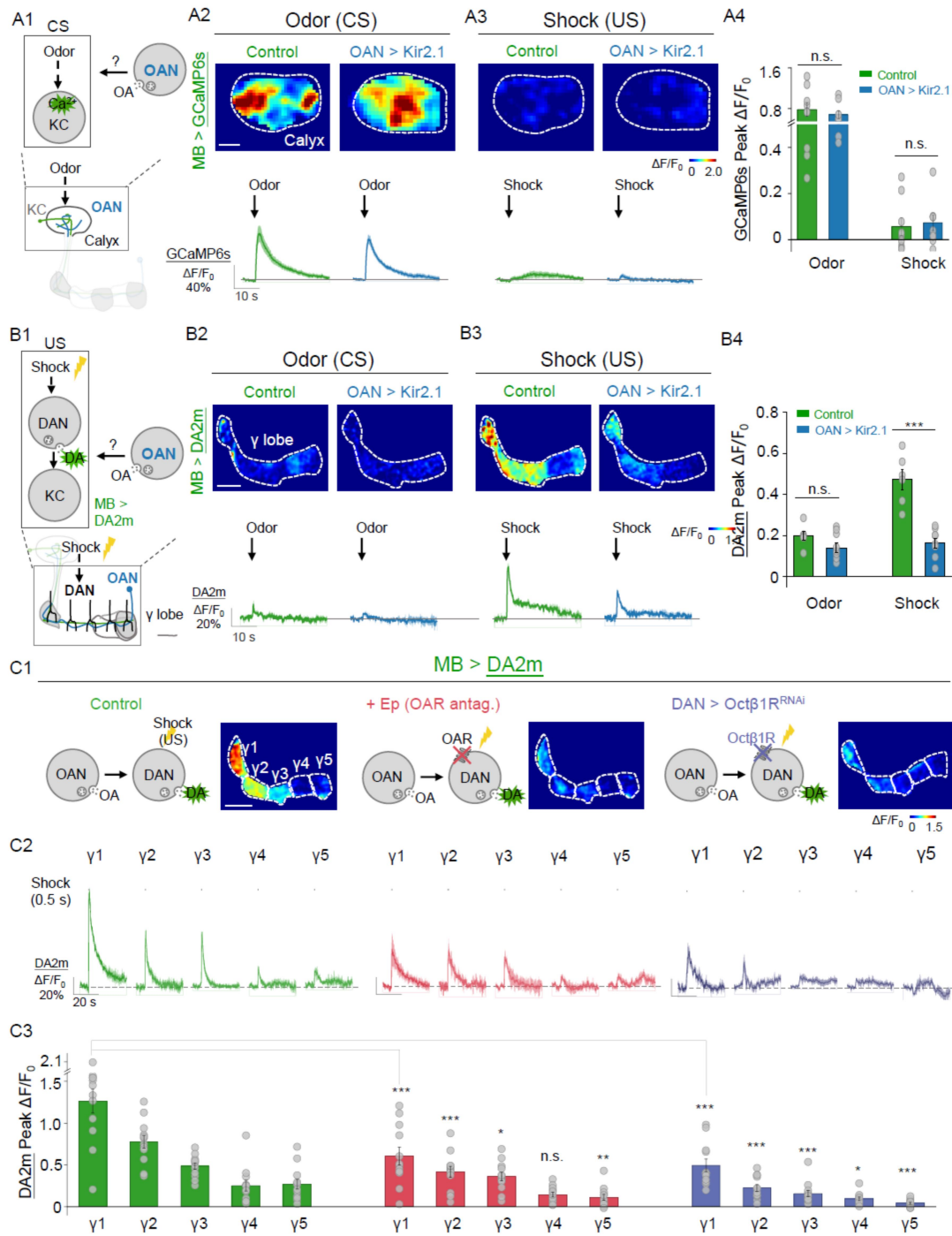
783 (C-E) Schematic diagram (C) depicting the *in vivo* 2PM imaging setup, a representative

784 fluorescence image (D), and the experimental protocol (E) in which odor-induced changes in

785 ACh3.0 fluorescence (MB247-LexA-driven) in the γ1-γ5 compartments were measured before

786 (pre), during, and after (post) pairing.
787 (F-G) Representative pseudocolor images (F1, G1) and average traces (F2, G2) of
788 odor-evoked ACh3.0 responses measured in the γ 1- γ 5 compartments before and after pairing
789 in response to the CS+ odorant (F) and CS- odorant (G) in control flies (top) and OAN-silenced
790 (OAN > Kir2.1) flies (bottom). F3 and G3: Summary of the change in odor-evoked ACh release
791 (post/pre responses) after pairing in response to the CS+ odorant (F3) and CS- odorant (G3) in
792 control flies and OAN > Kir2.1 flies; n = 6-9 flies/group.
793 *p < 0.05, ***p < 0.001, and n.s., not significant (unpaired Student's t-test). Scale bar= 20 μ m.
794

ORIGINAL UNEDITED MANUSCRIPT



796

797 **Figure 5. OA is required for driving DA release in response to aversive stimuli.**

798 (A) Schematic diagram (A1) showing the strategy for measuring intracellular calcium signals in
 799 the MB (MB247-LexA-driven) by expressing GCaMP6s in either control flies or OAN > Kir2.1
 800 flies, in response to the conditioned stimulus (CS) or unconditioned stimulus (US). Also shown

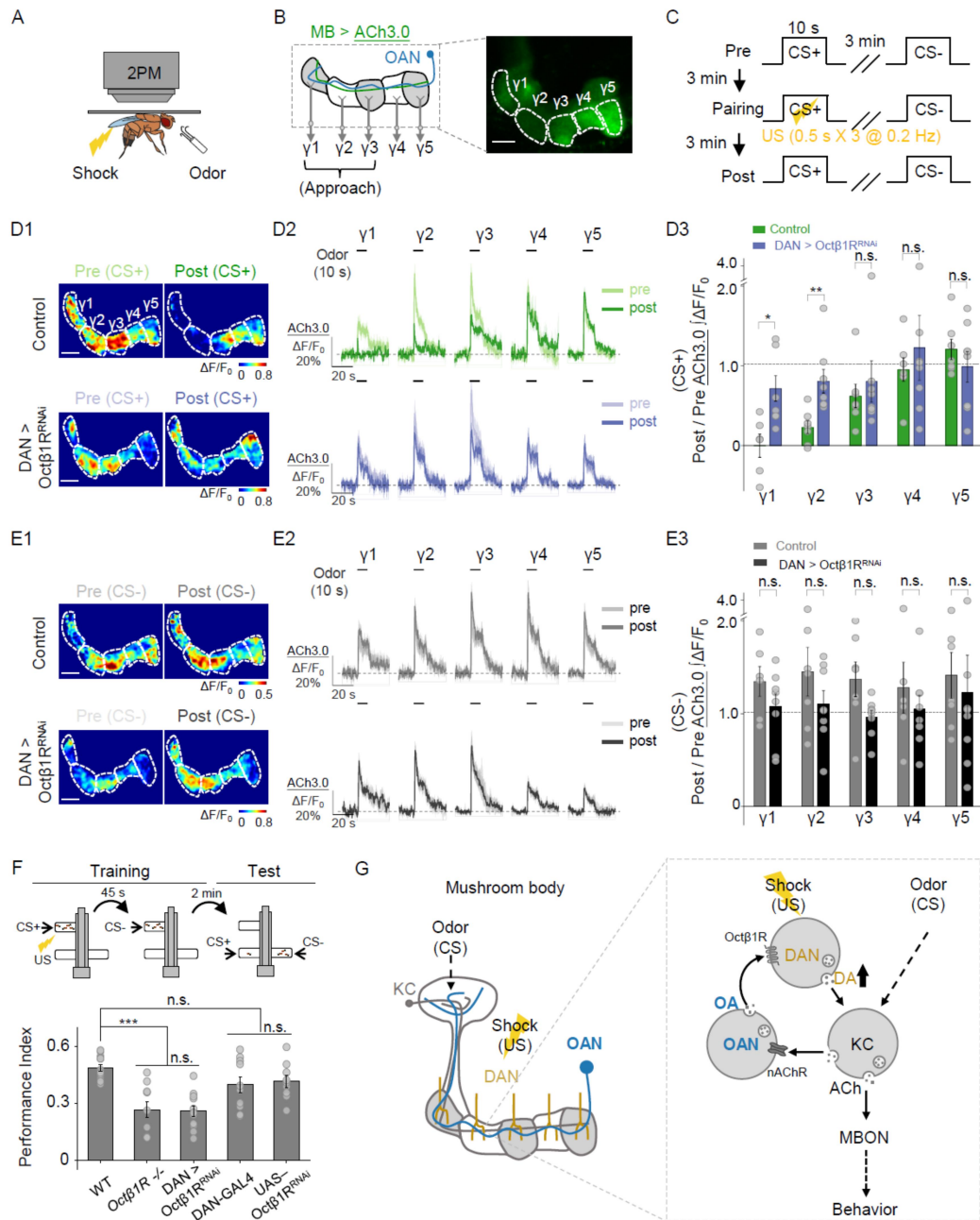
801 are representative pseudocolor images (A2-A3, top), traces (A2-A3, bottom), and summary
802 (A4) of calcium signals measured in the calyx in response to odor (A2) or electrical body shock
803 (A3); n = 9 flies/group.

804 (B) Schematic diagram (B1) showing the strategy for measuring dopamine (DA) signals in the
805 MB (R13F02-LexA-driven) by expressing the DA2m sensor in either control flies or OAN >
806 Kir2.1 flies, in response to the CS or US. Also shown are representative pseudocolor images
807 (B2-B3, top), traces (B2-B3, bottom), and summary (B4) of DA release measured in the γ lobe
808 in response to in response to odor (B2) or electrical body shock (B3); n = 6-9 flies/group.

809 (C) C1: Schematic diagrams (C1) showing DA2m imaging in flies and representative
810 pseudocolor images whose brain was bathed in saline (left) or saline containing 100 μ M Ep
811 (middle), or DAN > Oct β 1R^{RNAi} (TH-GAL4-driven) flies (right) in response to body shock stimuli.
812 Also shown are representative traces (C2) and the summary (C3) of DA release measured in
813 the γ 1- γ 5 compartments; n = 12 flies/group.

814 *p < 0.05, **p < 0.01, ***p < 0.001, and n.s., not significant (unpaired Student's t-test). Scale
815 bar= 20 μ m.

ORIGINAL UNEDITED MANUSCRIPT



817

818 **Figure 6. OA acts on DANs via the Oct β 1R receptor to modulate aversive learning.**

819 (A-C) Schematic diagram (A) depicting the *in vivo* 2PM imaging setup, a representative
 820 fluorescence image (B), and the experimental protocol (C) in which odor-induced changes in
 821 ACh3.0 (MB247-LexA-driven) fluorescence were measured in the γ 1- γ 5 compartments before,
 822 during, and after pairing.

823 (D-E) Representative pseudocolor images (D1, E1), average traces (D2, E2), and summary
824 (D3, E3) of odor-evoked ACh3.0 responses measured in the γ 1- γ 5 compartments in response
825 to the CS+ odorant (D) and CS- odorant (E) in the indicated groups; n = 6-8 flies/group.
826 (F) Schematic diagram depicting the T-maze protocol (top) and summary of the performance
827 index (bottom) measured in the indicated groups; n = 9-12 for each group.
828 (G) Model depicting the proposed mechanism for how OA acts on DANs in the MB to modulate
829 aversive learning. MBON, mushroom body output neuron.
830 *p < 0.05, **p < 0.01, ***p < 0.001, and n.s., not significant (unpaired Student's t-test). Scale
831 bar = 20 μ m.
832

ORIGINAL UNEDITED MANUSCRIPT